Search for Two Nucleon States by the ^<12>C (γ, pn) ^<10>B Reaction(I. Nuclear Physics)

著者	Hirose K., Chiba M., Inoue M., Kanda H., Kino K., Konno O., Maeda K., Miyase H., Ohtsuki T., Suda T., Takahashi K., Tamae T., Terasawa T., Tsubota H., Utoyama M., Wakamatsu M., Yamaguchi Y., Yamazaki H., Yuuki H.
journal or publication title	核理研研究報告
volume	35
page range	23-29
year	2002-11
URL	http://hdl.handle.net/10097/31009

(LNS Experiment : #2351)

Search for Two Nucleon States by the $^{12}C(\gamma, pn)^{10}B$ Reaction

K. Hirose[1], M. Chiba[1], M. Inoue[2], H. Kanda[1], K. Kino[2]*, O. Konno[2]†, K. Maeda[1], H. Miyase[1], T. Ohtsuki[2], T. Suda[3], K. Takahashi[1], T. Tamae[2], T. Terasawa[2], H. Tsubota[1], M. Utoyama[1], M. Wakamatsu[1], Y. Yamaguchi[1], H. Yamazaki[2] and H. Yuuki[2]

[1]*Physics Department, Graduate School of Science, Tohoku University, Sendai 980-8578*
[2]*Laboratory of Nuclear Science, Tohoku University, Sendai 982-0826*
[3]*Institute of Physical and Chemical Research, 2-1 Hirosawa, Wako 351-0098*

We performed the $^{12}C(\gamma, pn)$ experiment using tagged photons in an energy range from 30 to 120 MeV. Protons and neutrons were detected by a range telescope and NE213 liquid scintillators, respectively. Missing energy spectra of the $^{12}C(\gamma, pn)$ reaction were deduced to search for the two nucleon excited states. In this report, we show the experimental setup for the $^{12}C(\gamma, pn)$ reaction using the tagged photon beams. The preliminary results are shown and discussed. The data analysis is in progress.

Real-photon induced nuclear reactions in an energy range from the giant dipole resonance (GDR) to near the pion threshold have been extensively studied at the Laboratory of Nuclear Science (LNS), Tohoku University [1, 2]. The characteristic features of the photonuclear reactions in this energy region are excitations of the giant resonance (GR), one-nucleon direct-knockout (DK) and photon absorption by a correlated nucleon pair due to the meson exchange current (MEC). In these experiments, we have shown the MEC plays a dominant role in the photon absorption process above the GR region [3-9]. Although we have tried to investigate the two nucleon excitations by $(\gamma, 2N)$ reactions, sufficient data have not been obtained for the detailed discussion.

The $^{12}C(\gamma, pn)$ experiment was carried at the experimental Hall-1 of LNS. Electron beams from the 300-MeV Linear accelerator are stretched by the stretcher and booster ring (STB-ring). They are delivered to the experimental Hall-1 through a beam transport line called Beam Line Five (BL-V). As shown in Fig.1, the photon tagging system (TAGGER) is located at the end of the beam transport line to the Hall-1. The electron beams produce photons in a bremsstrahlung target placed at the entrance of the TAGGER.

*Present address: Research Center for Nuclear Physics, Osaka University, Mihogaoka, Ibaraki, Osaka 567-0047

‡Present address: Ichinoseki National College of Technology, Takanashi, Hagisho, Ichinoseki 021-8511

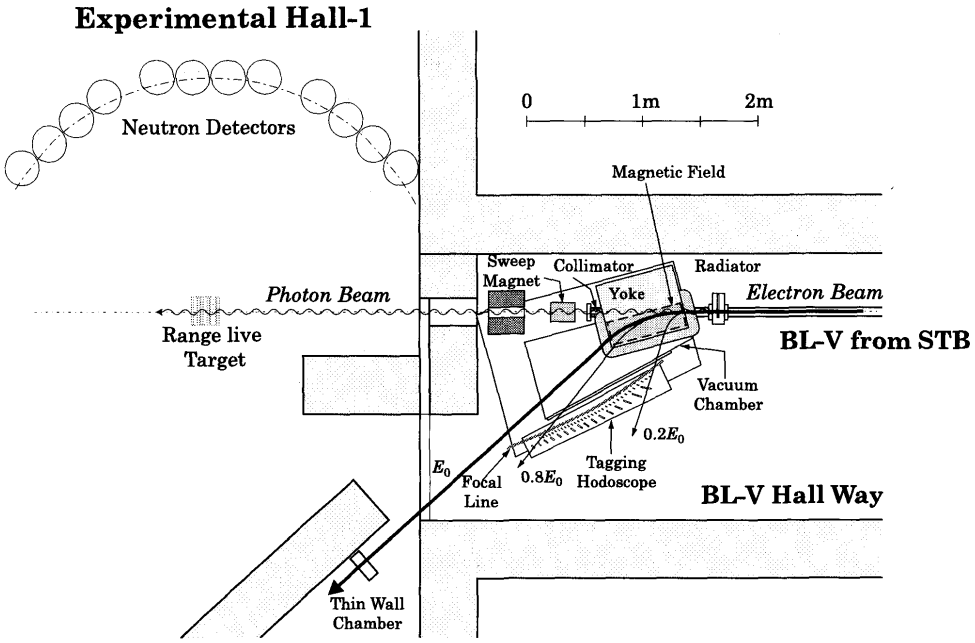

Fig.1. Layout of the photon tagging system and the neutron detector setup for (γ, pn) experiments.

The TAGGER is composed of a bremsstrahlung radiator, a dipole magnet and electron counters. The incident electrons impinge on a gold foil ($3\,\mu m$) in a radiator box. The bremsstrahlung photons are produced in the radiator. The energy of the post-bremsstrahlung recoil electron is analyzed in a magnetic field. The tagged photon energy is determined by,

$$E_\gamma = E_0 - E_e - E_{recoil} \quad (1)$$

where E_0 and E_e are the incident and outgoing electron energies, respectively. Since the recoil energy E_{recoil} is negligible, the tagged photon energy E_γ is determined by E_0 and E_e.

A hodoscope was used for the electron counter at the focal plane. It consists of 64-channel tagging counters (TC) and 16-channel tagging backup counters (BC), covering the energy range from 0.2 to 0.8 E_0. They are made of plastic scintillator. Each of them has an equal energy spread of $\Delta E/E_0 \approx 9.3 \times 10^{-3}$.

A range telescope was used for a proton detector. It consists of eight pieces of NE110 plastic scintillators. Each plastic scintillator has the dimensions of $10 \times 10 \times 1$ cm^3. The range telescope was used as an active target. The natural carbon in the plastic scintillator is the target whose thickness is 7.8 g/cm^2. Advantages of the active target is the large acceptance for protons. Electrons detected in the telescope are discriminated by the range and the light-output data. A plastic veto was placed downstream of the range telescope to reduce high energy electrons. In order to know the proton detection efficiency, GEANT3 was employed. The (γ, pn) events were generated by the ^{2}H(γ, pn) kinematics. Simulated data was analyzed in the same way as the data analysis. In Fig. 2, we show the estimated efficiency, where the proton and neutron emission angle were $\theta_p \approx 120°$, $\theta_n \approx 43°$, respectively. Open circles show the total efficiency, where the threshold energy is 5 MeV. Closed squares show the efficiency when the proton was stopped in one layer and closed triangles indicate the efficiency when the proton was detected in two layers.

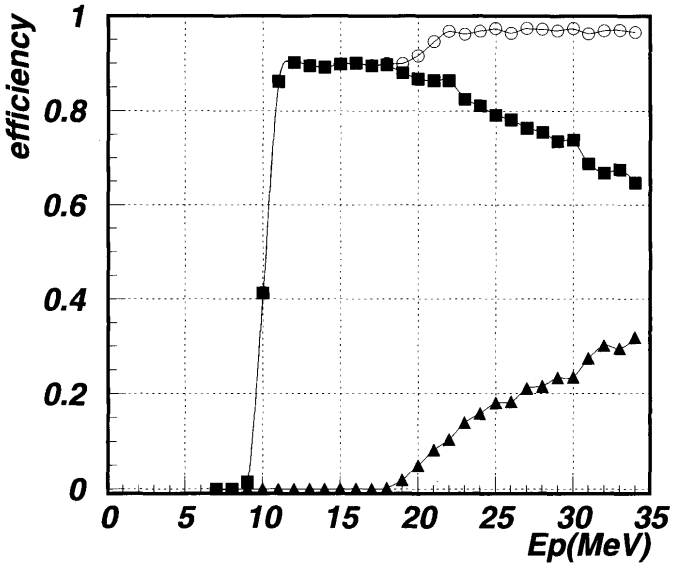

Fig.2. Calculated efficiency. Closed squares and triangles show the efficiency when the proton is stopped in one and two layers in the telescope, respectively. Open circles show those sum.

Neutrons were detected by twelve NE213 liquid-scintillator detectors. The container was fabricated from an aluminum cylinder. The internal size was 300 mm long and 200 mm ϕ. The neutron detectors were placed perpendicular to the ground, at laboratory angles from $\theta_{lab} \approx 35^\circ$ to 140°. A time-of-flight (TOF) method was employed to determine the neutron kinetic energy. The average flight path was 1.7 m. The timing uncertainty of the neutron detector system was $\Delta t \approx 2.54$ nsec (FWHM). It comes from the neutron detector size. The angle (θ_{ND}) and the flight path (L) of neutron detectors are tabulated in Table 1.

Table 1. The angles and flight paths of neutron detectors.

Detector	L (m)	θ_{ND} (deg)	Detector	L (m)	θ_{ND} (deg)
ND1	1.75	35.1	ND7	1.62	92.2
ND2	1.69	43.3	ND8	1.65	101.0
ND3	1.67	52.1	ND9	1.74	113.7
ND4	1.70	60.7	ND10	1.69	122.2
ND5	1.68	74.7	ND11	1.66	131.1
ND6	1.63	83.5	ND12	1.68	140.0

Plastic scintillators were installed in front of the neutron detectors to veto charged particles. Pulse shapes from the neutron detector were analyzed by a dual-gate charge comparison (DCC) method to separate γ-rays. A typical two dimensional display for the DCC is shown in Fig.3. The horizontal axis indicates the ratio of the ADC channel for narrow (40 nsec) gate to that for wide (400 nsec) gate. The vertical axis indicates the ADC channels for wide gate. Peaks of neutrons and γ -rays were fitted with Gaussian. The neutrons were separated from the γ -rays at the point where two Gaussians cross each other. The number of missing neutrons in this procedure depends on the gate position and the pulse height. Figure 4 shows the pulse height dependence of the neutron selection efficiency.

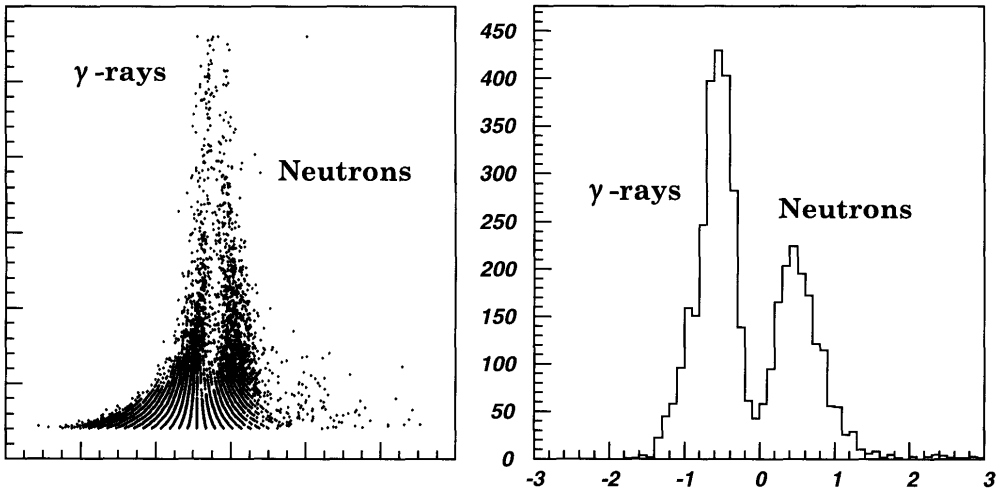

Fig.3. Separation of neutrons and γ-rays with the dual-gate charge comparison (DCC) method. The horizontal axis indicates the ratio of the ADC channel for narrow (40 nsec) gate to that for wide (400 nsec) gate. The vertical axis indicates the ADC channels for wide gate. The projection to the horizontal axis is also shown, where the threshold position is 6.0 MeV.

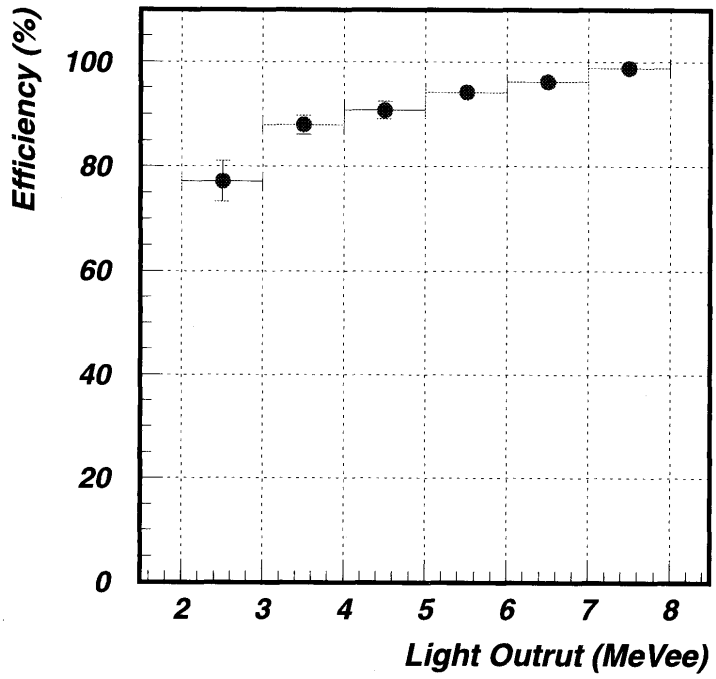

Fig.4. The neutron selection efficiency.

The neutron detection efficiency was calculated by a computer code SCINFUL [10,11]. It is designed to calculate a full response for the NE213 (liquid) scintillator. The detection efficiency wes obtained by integrating the response function above the threshold. The detection efficiency of the NE213 liquid scintillator detector used in this experiment is shown in Fig.5 as a function of the neutron energy for four different thresholds. They are 2.5, 5, 7.5, and 10 MeVee, where MeVee represents an electron equivalent energy unit.

Signals from the tagging counters are processed by sixteen 4-channel Quad Tag Modules (QTM), which accept four independent linear signals from the TC. They are amplified and discriminated in the QTM. The TC signals are strobed by a timing signal from the corresponding BC. The QTMs produce

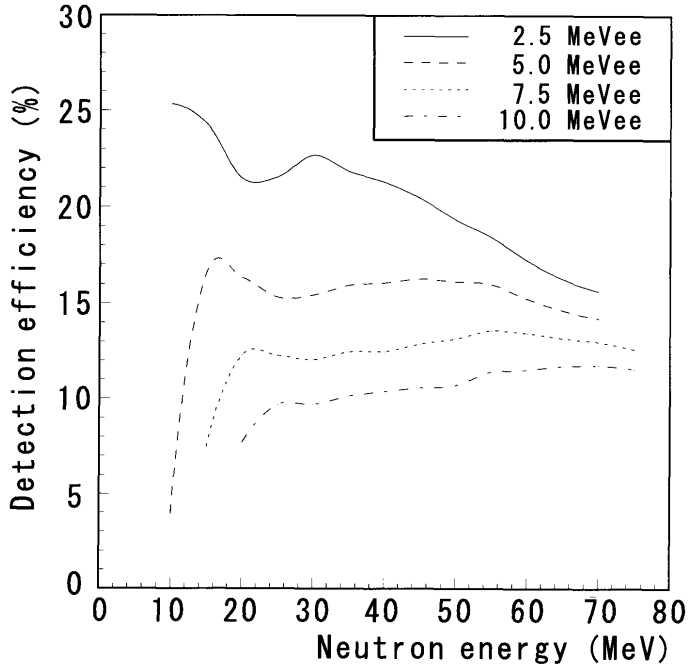

Fig.5. The neutron detection efficiency of the NE213 liquid scintillator detector for different thresholds of 2.5 (solid line), 5 (dashed line), 7.5 (dotted line), and 10 MeVee (dashed-dotted line).

four strobed TC signals and their logical sums ([Σ4]). The trigger signal of the TAGGER side is,

$$[\Sigma 64] = \sum_{i=1}^{16} [\Sigma 4]_i = [\Sigma 4]_1 \oplus [\Sigma 4]_2 \oplus \cdots \oplus [\Sigma 4]_{16} \quad (2)$$

$$= \sum_{i=1}^{64} [\mathrm{TC}]_i \quad (3)$$

where $[\Sigma 4]_i$ is the i-th QTM strobed sum. The NIM bins for the QTMs are gated by a beam gate to be free from the beam injection noise.

The strobed TC signals are used for input signals of a 64-channel fast TAGGER processor (FTP64), which produces 16-channel TDC stop signals. The FTP64 enables to reduce the TDC channels and simplify the electronics.

The event trigger signal ([ET]) is,

$$[\mathrm{ET}] = [\Sigma 64] \otimes ([\mathrm{ND}] \otimes [\mathrm{RT}]) \otimes \overline{[\mathrm{veto}]} \quad (4)$$

where [ND] and [RT] are logical sums of neutron detectors and the range telescope respectively, and $\overline{[\mathrm{veto}]}$ is any veto signal.

A CAMAC+PC/Windows-NT™ was used for the data acquisition [12]. The data are collected through a Kinetic-3922 CAMAC crate controller and a Kinetic-2927 PCI/bus interface. When the collector receives a LAM signal from the CAMAC, it starts to transfer the raw data from the CAMAC. The recorder writes the data from the collector on a shared memory. The raw data are also stored on a hard disk for an online analysis and DAT for mass storage. The data server transmits the collected data via a TCP/IP socket to the back-end computers for the online analysis. The analyzer in the back-end computer system displays the data on the monitor screen and refreshes the screen every few seconds. These processes are controlled by the process controller, which is operated via a visual interface panel

displayed on the monitor screen.

The energy of protons was calibrated using electrons, which pass through 1.0 cm thick plastic scintillator, and make 1.7 MeV energy loss (1 e^- peak) and 2 e^- peak at 3.5 MeV. The energy resolution was derived from widths of these peaks.

The energy of neutrons was determined using the TOF method. The time resolution of the neutron detector system was about 2.54 nsec. The energy resolution was about 2 MeV at 20 MeV.

The events including the multiple hits of tagging counters were excluded at the early stage of the analysis. The coadjacent hits in TCs are considered to be produced by one electron. In this case the photon energy is assumed to be the mean value of two TCs.

The protons in the range telescope are selected with the following condition;

- If the energy loss of i-th layer $E_i \geq 1.0$ MeV, this layer is regarded as 'hit'.
- There is only one *hit*-layer and $E_i \geq 10.0$ MeV.
- There are two continuously *hit*-layers and $(E_i + E_{i+1}) \geq 15.0$ MeV.
- There are more than three continuously *hit*-layers and the energy losses of each layer lying between first *hit*-layer and last one are greater than 7.5 MeV.

Figure 6 shows a missing energy spectrum $E_{\mathrm{miss}} = E_\gamma - E_\mathrm{n} - E_\mathrm{p}$ at $\theta_\mathrm{n} = 43.3^\circ \pm 6.8^\circ$. The Q-value of the $^{12}\mathrm{C}(\gamma, \mathrm{pn})$ reaction is -27.4 MeV. We can see the steep rise near the $^{12}\mathrm{C}(\gamma, \mathrm{pn})$ threshold. The peak structure around $E_{\mathrm{miss}} = 30$ MeV is corresponds to the ground state of the residual ^{10}B. Although we are interested in the bump above 40 MeV, there is no clear structure in this missing energy region.

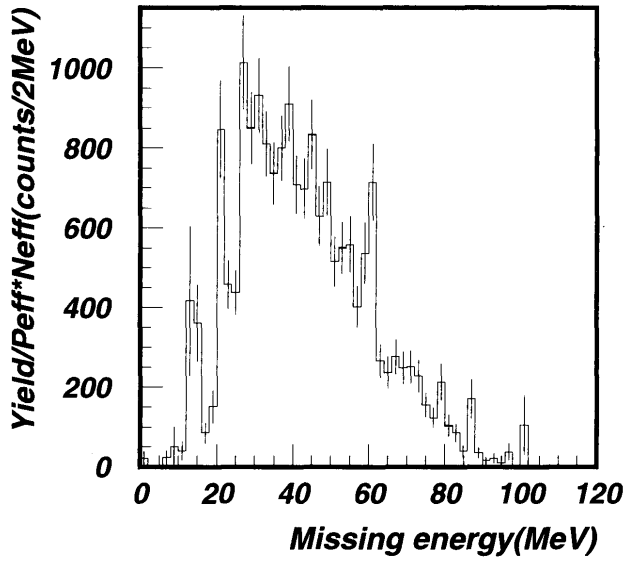

Fig.6. Preliminary missing energy spectrum $E_{\mathrm{miss}} = E_\gamma - E_\mathrm{p} - E_\mathrm{n}$. $E_\gamma \geq 44$ MeV, $\theta_\mathrm{n} = 44.3^\circ \pm 6.8^\circ$

We performed the $^{12}\mathrm{C}(\gamma, \mathrm{pn})$ experiment using tagged photons in the photon energy range from 30 to 120 MeV. The protons and the neutrons emitted at the final stage were detected by the range telescope and the NE213 liquid scintillators, respectively. The protons were selected by the range and the energy loss information in the range telescope. The dual-gate charge comparison method was employed for the neutron selection. We deduced the preliminary spectra of the missing energy. The

missing energy spectra indicate the steep rise near the reaction threshold. The data analysis is in progress.

References

[1] T. Tamae *et al.* : Nucl. Instr. and Meth. **A264**, (1988) 173.

[2] T. Terasawa *et al.* : Nucl. Instr. and Meth. **A248** (1986) 429.

[3] P.D. Harty *et al.* : Phys. Rev. **C37** (1988) 13.

[4] T. Suda *et al.* : J. Phys. Soc. Jpn. **57** (1988) 5.

[5] J. Yokokawa *et al.* : J. Phys. Soc. Jpn. **57** (1988) 695.

[6] J.A. Eden *et al.* : Phys. Rev. **C44** (1991) 753; Erratum Phys. Rev. C46 (1992) 385.

[7] D.A. Sims *et al.* : Phys. Rev. **C45** (1992) 479.

[8] S. Ito *et al.* : Nucl. Instr. and Meth. **A354** (1995) 475.

[9] K. Mon *et al.* : Phys. Rev. **C51** (1995) 2611.

[10] J.K. Dickens: ORNL-6436, Oak Ridge National Laboratory, 1988; Nucl. Instr. and Meth. **A401** (1997) 365.

[11] S. Meigo: Nucl. Instr. and Meth. **A401** (1997) 365.

[12] M. Kawabata and M. Mutoh: Nucl. Instr. and Meth. **A454** (2000) 460.